

# Cosmological Structures behind the Milky Way

Renée C. Kraan-Korteweg

Departamento de Astronomía, Universidad de Guanajuato,

Apartado Postal 144, Guanajuato GTO 36000, México

Astronomy Department, University of Cape Town<sup>1</sup>,

Rondebosch 7700, South Africa

kraan@circinus.ast.uct.ac.za, <http://mensa.ast.uct.ac.za/~kraan>

## Abstract

*This paper provides an update to the review on extragalactic large-scale structures uncovered in the Zone of Avoidance (ZOA) by Kraan-Korteweg & Lahav 2000, in particular in the Great Attractor (GA) region. Emphasis is given to the penetration of the ZOA with the in 2003 released near-infrared (NIR) 2MASS Extended Source Catalog. A comparison with deep optical searches confirms that the distribution is little affected by the foreground dust. Galaxies can be identified to extinction levels of over  $A_B \gtrsim 10^m$  compared to about  $3^m$  in the optical. However, star density has been found to be a strong delimiting factor. In the wider Galactic Bulge region ( $\ell = 0^\circ \pm 90^\circ$ ) this does not hold and optical surveys actually probe deeper (see Fig. 9). The shape of the NIR-ZOA is quite asymmetric due to Galactic features such as spiral arms and the Bulge, something that should not be ignored when using NIR samples for studies such as dipole determinations.*

*Various systematic surveys have been undertaken with radio telescopes to detect gas-rich galaxies in the optically and NIR impenetrable part of the ZOA. We present results from the recently finished deep blind HI ZOA survey performed with the Multibeam Receiver at the 64 m Parkes telescope ( $v \lesssim 12700 \text{ km s}^{-1}$ ). The distribution of the roughly one thousand discovered spiral galaxies within  $|b| < 5^\circ$  clearly depict the prominence of the Norma Supercluster. In combination with the optically identified galaxies in the ZOA, a picture emerges that bears a striking resemblance to the Coma cluster in the Great Wall in the first redshift slice of the CFA2 survey (de Lapparent, Geller & Huchra 1986): the rich Norma cluster (ACO 3627) lies within a great-wall like structure that can be traced at the redshift range of the cluster over  $\sim 90^\circ$  on the sky, with two foreground filaments – reminiscent of the legs in the famous stick man – that merge in an overdensity at slightly lower redshifts around the radio galaxy PKS 1343–601 (see Figs. 14 & 16).*

## 1 Introduction

The absorption of light due to dust particles and the increase in star density close to the Galactic Equator and around the Galactic Bulge creates a “Zone

---

<sup>1</sup>since January 2005

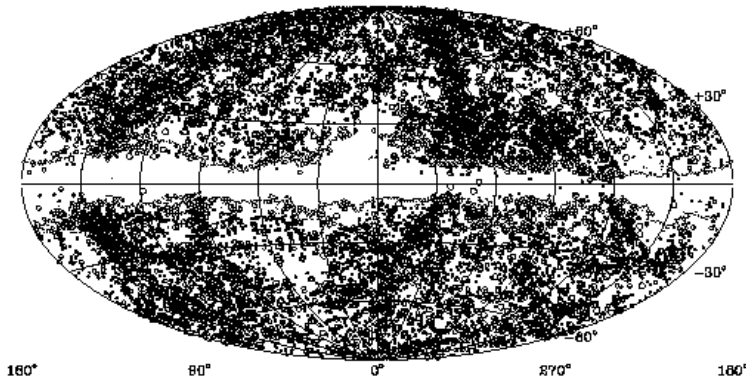


Figure 1: Aitoff equal-area projection in Galactic coordinates of galaxies with  $D \geq 1'.3$ . The galaxies are diameter-coded. The contour marks absorption in the blue of  $A_B = 1^m0$  as determined from the Schlegel, Finkbeiner & Davis (1998) dust extinction maps. Figure from KK&L2000.

of Avoidance” in the distribution of galaxies, the size and shape of which depends on the wavelength at which galaxies are sampled. Figure 1 shows a complete sample of optically cataloged galaxies in an Aitoff projection in Galactic coordinates (see Kraan-Korteweg & Lahav 2000 for details; henceforth KK&L2000). The broad band void of galaxies takes up about 20% of the sky. Its form is like a near-perfect negative of the optical light distribution as depicted in the famous composite by Lundmark (1940), and is well traced by the dust (see contour in Fig. 1).

The ZOA has, with few exceptions, been avoided by astronomers studying the extragalactic sky because of the inherent difficulties in determining the physical parameters of galaxies lying behind the disk of our Galaxy – if they can be identified at all. The effect of absorption and star-crowding is illustrated in a simulation made by Nagayama (2004) which is reproduced in Fig. 2. The images are based on observations made with the Japanese 1.4 m Infrared Survey Facility (IRSF) at the Sutherland observing site of the South African Astronomical Observatory. The camera on the IRSF has the ability to simultaneously take  $J$ ,  $H$ , and  $K$  data with a field of view of  $8' \times 8'$ .

The left-hand panel shows a combined  $JHK$  field in the Hydra cluster where absorption is negligible and star-crowding a minor problem. Subjecting this image to a foreground extinction of  $A_B = 12^m$  which in the NIR bands  $JHK$  reduces to a mere  $2^m5$ ,  $1^m7$  and  $1^m1$  respectively (see Sect. 3 for details) results in the image of the middle panel. While the originally small and faint galaxies are lost completely, the larger galaxies are smaller in size, of lower surface-brightness, and redder. A further difficulty in identifying galaxies and determining their properties is star-crowding. To illustrate this, Nagayama then combined this artificially absorbed field with a field in the surroundings of the radio galaxy PKS 1343–601 at low Galactic latitudes

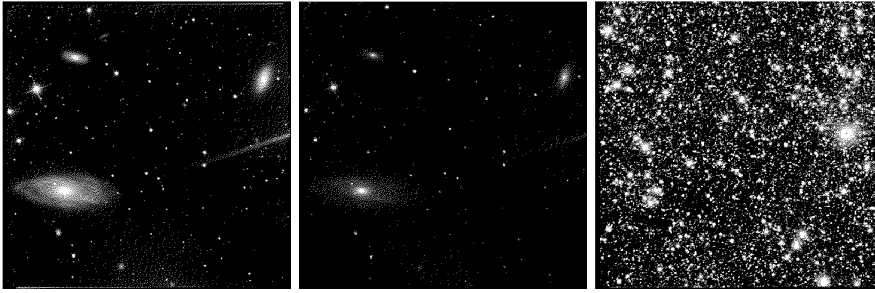


Figure 2: Left: A *JHK* image of  $8' \times 8'$  obtained with the Japanese IRSF of the Hydra galaxy cluster. Middle: simulation of same field seen through an obscuration layer of  $12^m0$ ,  $2^m5$ ,  $1^m7$ , and  $1^m1$  of extinction in the *BJHK* bands respectively. Right: previous field now positioned in the area of the low latitude radio galaxy PKS 1343–601. Figure adopted from Nagayama 2004.

( $\ell = 309^\circ.7, b = +1^\circ.8$ ), also obtained with IRSF. This is reproduced in the right-hand panel of Fig. 2. Here, the recognition of even the intrinsically largest galaxies is hard when knowing where the galaxies are located (see panels to the left). Further examples of extinction and star-crowding effects can be found on <http://www.z.phys.nagoya-u.ac.jp/~nagayama/hydra>. This site also shows some examples of real galaxy candidates detected behind this thick obscuration and star layer.

The simulation clearly demonstrates why the incentive was low to map and investigate galaxies, their properties and their distribution in space in the ZOA. However, with the realization that galaxies are located predominantly in clusters, sheets and filaments, leaving large areas devoid of luminous matter, came the understanding that a consensus of galaxies of the “whole sky” is required when addressing various cosmological questions related to the dynamics of the local Universe.

The closest superclusters such as the Local Supercluster, the Centaurus Wall, the Perseus-Pisces chain, the Great Attractor – a large mass overdensity of about  $5 \cdot 10^{16} \mathcal{M}_\odot$  that was predicted from the systematic infall pattern of 400 ellipticals (Dressler et al. 1987) – all are bisected by the Milky Way, making a complete mapping and determination of their extent and dynamics impossible. Moreover, the irregular distribution of mass induces systematic flow patterns over and above the uniform Hubble expansion of the Universe. This effect is seen in the peculiar motion of the Local Group with respect to the Cosmic Microwave Background (CMB; e.g. Kogut et al. 1993). Such systematic flow patterns were first mapped within the Virgo Supercluster (Tonry & Davis 1981) and later on a much larger scale later in the Great Attractor region. It might even perturb the motions of galaxies in a volume all the way out to the Shapley Concentration, including the GA as a whole, though this still remains controversial (e.g. Kocevski, Mullis, & Ebeling 2004; Lucey, Radburn-Smith & Hudson, 2005; Hudson et al. 2004).

Kolatt, Dekel & Lahav (1995), have shown that the mass distribution of the inner ZOA ( $b \pm 20^\circ$ ) as derived from theoretical reconstructions of the density field is crucial to the derivation of the gravitational acceleration of the LG. This not only concerns hidden clusters, filaments, and voids. Nearby massive galaxies may also contribute significantly to the dipole and many of the nearby luminous galaxies do actually lie behind the Milky Way (e.g. Kraan-Korteweg et al. 1994). Moreover, a hidden Andromeda-like galaxy will influence the internal dynamics of the LG, its mass derivation and the present density determination of the Universe from timing arguments (Peebles 1994).

For our understanding of velocity flow fields, in particular the Great Attractor, the ZOA constitutes a severe barrier. The various 2 and 3-dimensional reconstruction methods find the flow towards this GA to be due to a quite extended region of moderately enhanced galaxy density centered on the Milky Way (about  $\sim 40^\circ \times 40^\circ$ , centered on  $\ell, v, b \sim 320^\circ, 0^\circ, 4500 \text{ km s}^{-1}$ ; see e.g. Fig. 1b in Kolatt et al. 1995). Although a considerable excess of galaxies is seen in that general region of the sky (Lynden-Bell & Lahav 1988; Fig. 1 here), no dominant cluster or central peak had been identified. Whether it existed and whether galaxies were fair tracers of the dynamically implicated mass distribution could not be answered, because a dominant fraction of the GA was hidden by the Milky Way.

For these reasons, various groups began projects in the last 10–15 years to try to unveil the galaxy distribution behind our Milky Way. Preliminary results, mainly based on optical, HI observations and follow-up of selected IRAS-PSC galaxy candidates, were presented at the first conference on this topic in 1994 (see Balkowski & Kraan-Korteweg (eds.) 1994, ASP Conf. Ser. 67). Meanwhile most of the ZOA has been probed in a “systematic” manner in “all” wavelength ranges of the electromagnetic spectrum (optical, near- and far-infrared, HI and X-ray), next to, and in comparison to, the reconstructed density fields in the ZOA. Many of these surveys and subsequent results are described in the proceedings of the second and third meeting on this topic (Kraan-Korteweg, Henning & Andernach (eds.) 2000, ASP Conf. Ser. 218; Fairall & Woudt (eds.) 2005, ASP Conf. Ser. 329).

A comprehensive overview on the then current status of all the ZOA projects was prepared in 2000 by Kraan-Korteweg & Lahav. It provides a detailed introduction on the motivation of ZOA studies, the status of and the results from the different survey methods, including a discussion on the limitations and selection effects of the various approaches, as well as how they complement each other. In this paper, I will build on the information given there, and concentrate mainly on new results, although a summary and an update on the results from deep optical galaxy searches and redshift follow-ups in the Great Attractor region is given in Sect. 2, as these are relevant to the discussions in the subsequent sections. Sect. 3 describes the enormous progress made in NIR-surveys with the release of the 2MASS Extended Source Catalog (2MASX) which contains 1.65 million galaxies or other extended sources over the whole-sky. It contains a discussion on the characteristics of this survey, in particular to penetrating the ZOA in comparison to optical surveys. Sect. 4 is

dedicated to the results obtained from the systematic HI-survey of the southern ZOA that was performed between 1997 and 2002 with the Multibeam Receiver at the 64 m Parkes radio telescope. Next to the instrument and survey technique, the newly uncovered galaxy distribution is discussed. The last section (Sect. 5) will then describe the emerging picture of the Great Attractor overdensity including the data obtained from the various ZOA survey methods.

## 2 Optical Galaxy Searches and the GA

Optical galaxy catalogs become increasingly incomplete for intrinsically large galaxies towards the Galactic Plane, because of the reduction in brightness and ‘visible’ extent by the thickening dust layer and the increase in star density (Fig. 2). However, this is a gradual effect. Deeper searches for partially obscured galaxies – fainter and smaller than existing catalogs – have been successfully performed on existing sky survey plates. Over 50 000 unknown galaxies were uncovered, resulting in a considerable reduction of the ZOA.

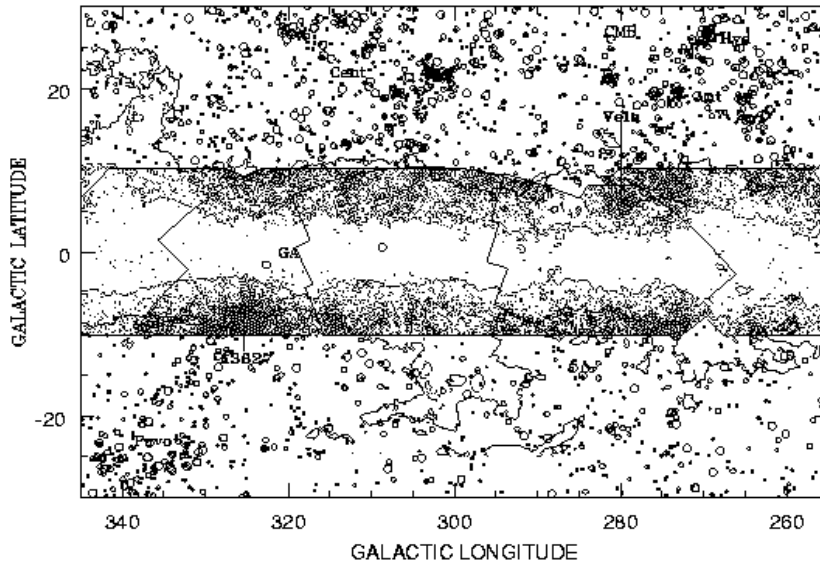


Figure 3: Distribution of Lauberts (1982) galaxies with  $D \geq 1'3$  (open circles) and galaxies with  $D \geq 12''$  (small dots) identified in the optical galaxy searches. The contours represent extinction levels of  $A_B = 1^m0$  and  $3^m0$ .

Fig. 3 gives an example of results obtained by our group in and around the Great Attractor region. This comprises (from right to left) the Vela region (Salem & Kraan-Korteweg, in prep.), Hydra/Antlia (Kraan-Korteweg 2000), Crux and Great Attractor (Woudt & Kraan-Korteweg 2001) and Scorpius (Fairall & Kraan-Korteweg 2000, 2005). Using a viewer with a 50 times

magnification on IIIaJ film copies of the ESO/SRC survey resulted in the identification of over 17 000 galaxies down to a diameter limit of  $D = 0'.2$  within Galactic latitudes of  $|b| \lesssim 10^\circ$  over a longitude range of  $250^\circ \lesssim \ell \lesssim 350^\circ$ . 97% were previously unknown. Their distribution is displayed in Fig. 3 together with earlier known galaxies. Note how the ZOA could be filled from  $A_B = 1^m0$ , the approximate completeness limit of previous catalogs, to  $A_B = 3^m0$ , with a few galaxies still recognizable up to extinction levels of  $A_B = 5^m0$ .

Distinct large-scale structures uncorrelated with the foreground obscuration can be discerned. The most extreme overdensity  $(\ell, b) \sim (325^\circ, -7^\circ)$  is found close to the core of the GA. It is centered on the cluster ACO 3627 (Abell, Corwin & Olowin 1989) and is at least a factor 10 denser compared to regions at similar extinction levels, and contains a significant larger fraction of brighter galaxies as well as elliptical galaxies. The prominence of this cluster had never been realized because of its location in the Milky Way. Within the Abell radius (defined as  $3 h_{50}^{-1}$  Mpc) of this cluster, a total of 603 galaxies with  $D \geq 0'.2$  have been identified, of which only 31 were cataloged before by Lauberts (1982).

Figure 4, a deeper *BRI* composite image obtained later by Woudt with the Wide Field Imager at the ESO 2.2 m telescope in la Silla (Woudt, Kraan-Korteweg & Fairall 2000), displays the center of this cluster in its full glory, despite the approximate 200 000 foreground stars. On this  $37' \times 37'$  image (left panel), even more galaxies can be identified than the 74 galaxies found in the same area on the IIIaJ fields. The cluster has, like the Coma cluster, two cD galaxies at its center. The richness of this cluster can be fully appreciated in the close-up in the right-hand panel with the there apparent large dwarf galaxy population (image centered on the right of center cD of the left panel).

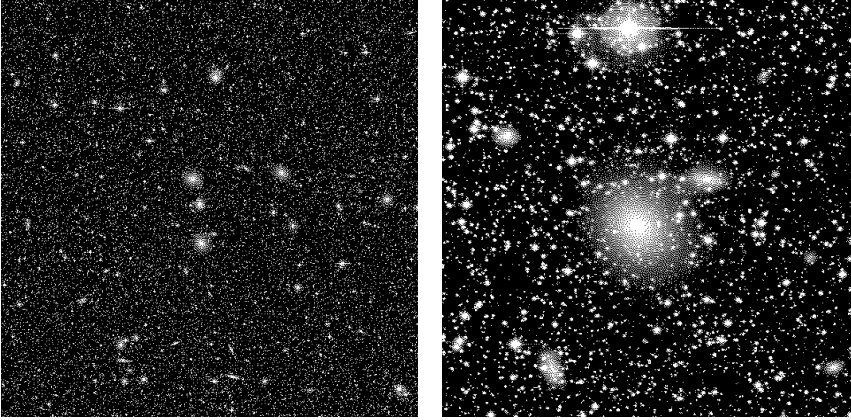


Figure 4: A *BRI* composite of the central  $37' \times 37'$  of the cluster ACO 3627 obtained with the WFI of the ESO 2.2 m telescope (left). Note the 2 dominant cD galaxies at the center of this cluster and the richness of the dwarf population in the close-up (4x) on the right. Figure from Woudt et al. 2000.

A quantification of the relevance of the newly uncovered galaxy distribution in context to known structures can be made when studying the completeness limits of the ZOA galaxy catalogs and correcting the observed parameters of the galaxies for the diminishing effects due to absorption applying the inverse Cameron (1990) laws. The latter provides equations to correct the observed magnitudes and diameters for their reduction as a function of extinction at their position behind the Milky Way. Kraan-Korteweg (2000) and Woudt & Kraan-Korteweg (2001) have shown that their catalogs are complete to  $D = 14''$  down to extinction levels of  $A_B \leq 3^m$ . Corrections for the apparently smallest galaxy at maximum extinction indicates that these surveys are complete for galaxies with extinction-corrected diameters of  $D^o = 1'.0$  down to  $A_B \leq 3^m$ .

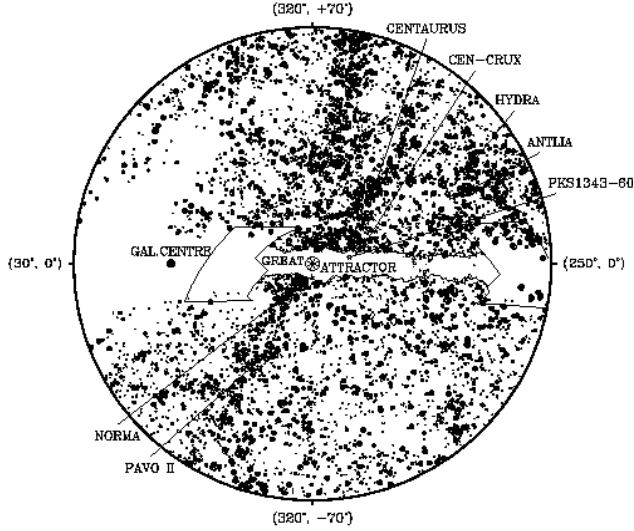


Figure 5: Equal area projection of galaxies with  $D^o \geq 1'.3$  and  $A_B \leq 3^m$  centered on the GA at  $(\ell, b) = (320^\circ, 0^\circ)$  within a radius of  $70^\circ$ . The galaxies are taken from the ESO, the UGC and the MGC, complemented by our ZOA catalogs. The extinction contour of  $A_B = 3^m$  is superimposed. Search areas in progress are indicated. Figure from Woudt & Kraan-Korteweg 2001.

Knowing that the combined ESO Lauberts (1982) catalog, the Uppsala General Catalog UGC (Nilson 1973), and the Morphological Catalog of Galaxies MGC (Vorontsov-Velyaminov & Archipova 1963-74) displayed in Fig. 1 are complete to  $D = 1'.3$  (Hudson & Lynden-Bell 1991), we can complement this merged whole-sky catalog down to  $A_B \leq 3^m$  with galaxies that would appear in these catalogs were they not lying behind the Milky Way, i.e. with  $D^o = 1'.3$ . This has been done in Fig. 5, in an equal area projection centered on the Great Attractor at  $(\ell, b) = (320^\circ, 0^\circ)$  and includes all galaxies with extinction-corrected diameters larger than  $D^o \geq 1'.3$  and  $A_B \leq 3^m$  from the

Hydra/Antlia, Crux and GA catalogs, next to the previously known galaxies from the ESO, UGC and MGC catalogs.

Figure 5 provides the most complete view of the optical galaxy distribution in the Great Attractor region to date. Comparing Fig. 5 with Fig. 1 demonstrates the reduction of the optical ZOA (over 50%). The final galaxy distribution not only shows the dominance of the ACO 3627 cluster, henceforth called the Norma cluster for the constellation in which it is located, but also displays a high galaxy density in the wider GA region on both sides of the Galactic Plane. Though the reduction of the ZOA is significant, optical approaches clearly do not fully succeed in penetrating the ZOA.

## 2.1 Velocity Distribution

Redshift coverage of the nearby galaxy population in the ZOA is essential in determining their impact on the local dynamics and also to identify the features that form part of the GA overdensity. We have aimed to obtain a fairly homogeneous and complete coverage of the (extinction-corrected) brighter and larger newly uncovered galaxies in the ZOA. Three distinctly different observational approaches were used: (i) optical spectroscopy for individual galaxies of high central surface brightness at the 1.9 m telescope of the SAAO (Kraan-Korteweg, Fairall, & Balkowski 1995; Fairall, Woudt, & Kraan-Korteweg 1998; Woudt, Kraan-Korteweg, & Fairall 1999), (ii) HI-line observations with the 64 m Parkes radio telescope for low surface brightness gas-rich spiral galaxies (Kraan-Korteweg, Henning & Schröder 2002; Schröder, Kraan-Korteweg & Henning, in prep.), (iii) low resolution, multi-fiber spectroscopy for the high-density regions with Optopus and MEFOS at the 3.6 m telescope of ESO, LaSilla (see Woudt et al. 2004 for MEFOS results). With the above observations, we typically obtain redshifts of 15% of the galaxies and can trace large-scale structures fairly well out to recession velocities of about  $20\,000\text{ km s}^{-1}$ .

The resulting velocity histograms are plotted in Fig. 6, separately for the three search areas. One glance immediately reveals the striking difference between the Hydra/Antlia, Crux and GA region, although all three have been sampled to approximately the same depth. The velocity distribution in Hydra/Antlia is overall quite shallow, with a peak at  $v \sim 2750\text{ km s}^{-1}$ , which corresponds to the extension of the Hydra/Antlia filament into the ZOA, and a broader overdensity at about  $6000\text{ km s}^{-1}$ , associated with the Vela overdensity ( $280^\circ, +6^\circ$ ), next to some higher velocity peaks.

In the Crux region, a broad concentration of galaxies is present from about  $3500$  to  $8500\text{ km s}^{-1}$ . This feature is already influenced by the GA overdensity. It is due to a wall-like structure that seems to connect the Norma cluster across the Centaurus-Crux, respectively the CIZA J1324.7–5736 cluster at  $(\ell, b, v) \sim (307^\circ, 5^\circ, 6200\text{ km s}^{-1})$  (Woudt 1998; Ebeling, Mullis & Tully 2002) to the Vela overdensity at  $(280^\circ, +6^\circ, 6000\text{ km s}^{-1})$  (see also Fig. 15 and 16).

The GA histogram, in comparison, is strongly dominated by the very high peak associated with the Norma cluster at  $4848\text{ km s}^{-1}$  (Kraan-Korteweg et



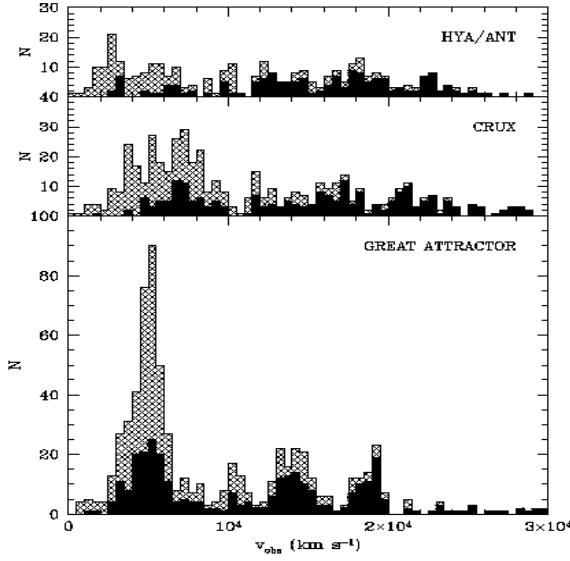


Figure 6: Velocity histograms in the Hydra/Antlia, Crux and GA regions. Dark shaded area correspond to the heliocentric velocities obtained with MEFOS, cross-hatched region includes the SAAO and Parkes observations as well as velocities from the literature. Figure from Woudt et al. 2004.

al. 1996; Woudt 1998) and the surrounding great wall-like structure in which it is embedded. The peak corresponds exactly to the predicted mean redshift of the Great Attractor. The Norma cluster, with a velocity dispersion of  $896 \text{ km s}^{-1}$ , has been found to have a virial mass of the same order as the Coma cluster (Kraan-Korteweg et al. 1996; Woudt 1998). This is confirmed independently by the X-ray observations with ROSAT (Böhringer et al. 1996) which finds the Norma cluster to be the 6th brightest ROSAT cluster in the sky. Simulations have furthermore shown that the well-known Coma cluster would appear the same as the Norma cluster if Coma were located behind the Milky Way at the location of the Norma cluster (Woudt 1998). The Norma cluster does not only seem the most likely candidate to define the core of the GA, it also seems to have superseded the well-known Coma cluster as being the nearest rich cluster to the LG, and therefore is an interesting cluster on its own, irrespective of its central position in the GA region.

A detailed dynamical analysis of the Norma cluster is in preparation (see Woudt 1998, Woudt et al. 2000, for preliminary results), as well as a precise determination of its distance (Woudt et al. 2005, Woudt et al., in prep.), in order to determine whether the Norma cluster, and therefore the GA as a whole, is at rest with respect to the CMB, or partakes in the earlier mentioned, still controversial flow towards to Shapley Concentration.

Besides the dominant peak due to the GA, the peak at  $14\,000 \text{ km s}^{-1}$  in the

lower panel of Fig. 6 is noteworthy. It is due to the Ara cluster (Woudt 1998; Ebeling et al. 2002) which together with the adjacent Triangulum-Australis cluster (McHardy et al. 1981) forms a larger overdensity referred to as a 'Greater Attractor behind the Great Attractor' by Saunders et al. (2000). They find a signature of this overdensity in the reconstructed IRAS galaxy density field.

## 2.2 Does the Norma Cluster Define the Core of the GA?

The emerging optical picture of the Great Attractor so far is that of a confluence of superclusters (the Centaurus Wall and the Norma supercluster) with the Norma cluster being the most likely candidate for the Great Attractor's previously unseen center. However, the potential well of the GA might be rather shallow and extended. Seen that the ZOA has not been completely reduced by deep optical surveys it is not inconceivable that further prospective galaxy clusters might be located at the bottom of the GA's potential well at extinction levels  $A_B \geq 3^m$  (Fig. 5).

Detecting clusters at higher extinction levels is not straightforward. The X-ray band is potentially an excellent window for studies of large-scale structure in the ZOA, because the Milky Way is transparent to the hard X-ray emission above a few keV, and because rich clusters are strong X-ray emitters. But although dust extinction and stellar confusion are unimportant in the X-ray band, photoelectric absorption by the Galactic hydrogen atoms – the X-ray absorbing equivalent hydrogen column density – does also limit detections close to the Galactic Plane. A systematic X-ray search for clusters in the ZOA ( $|b| \leq 20^\circ$ ) has been performed by Ebeling et al. (2002). They found only the above-mentioned Centaurus-Crux or CIZA J 1324.7–5736 cluster, as a previously unknown component, that might form part of the GA (see also Kocevski et al. 2004, Mullis et al. 2005), though it is by no means as centrally located in the GA, nor as massive as the Norma cluster.

Alternatively, a strong central radio source, such as PKS 1610–608 in the Norma cluster, could also point to unidentified clusters. Exactly such a source lies in the deepest layers of the Galactic foreground extinction ( $A_B = 12^m$ ) at  $(\ell, b, v) = (309.7^\circ, +1.7^\circ, 3872 \text{ km s}^{-1})$ . This strong radio source was suspected for a long time by Kraan-Korteweg & Woudt (1999) of being the principal member of an unknown rich galaxy cluster. An overdensity of galaxies around this massive galaxy had indeed been seen in blind HI-surveys, which are unaffected by extinction (see Sect. 4). Moreover, dedicated infrared studies in the surroundings of PKS 1343–601 also found an excess of galaxies (e.g. Kraan-Korteweg et al. 2005a in the *I*-band; Schröder et al. 2005 on DENIS *IHK*- images; and Nagayama et al. 2004, 2005, in *JHK*). The data are, however, not supportive of this being a rich massive cluster. This is consistent with the upper limit of X-ray emission determined from ROSAT data by Ebeling et al. 2002.

ACO 3627 thus remains the most likely candidate of constituting the central density peak of the potential well of the Great Attractor overdensity.

### 3 2MASS Galaxies and the ZOA

Observations in the near infrared (NIR) can provide important complementary data to other surveys. With extinction decreasing as a function of wavelength, NIR photons are much less affected by absorption compared to optical surveys. The  $I$ ,  $J$ ,  $H$  and  $K$  band extinction is only 45%, 21%, 14% and 9% compared to the optical  $B$  band – hence, as the mean longitude of the surveys in the respective wavebands increases, a progressively deeper search into thicker obscuration layers at lower Galactic latitudes is possible.

The NIR is sensitive to early-type galaxies – tracers of massive groups and clusters – which are missed in far infrared (FIR) surveys not discussed in this paper (but see KK&L2000) and HI surveys (Sect. 4). Moreover, recent star formation contributes only little to the NIR flux of galaxies (in contrast to optical and FIR emission) and therefore provides a better estimate of the stellar mass content of galaxies.

Two systematic near infrared surveys have been performed: DENIS, the DEep Near Infrared Southern Sky Survey, has imaged the southern sky from  $-88^\circ < \delta < +2^\circ$  in the  $I_c$  ( $0.8\mu\text{m}$ ),  $J$  ( $1.25\mu\text{m}$ ) and  $K_s$  ( $2.15\mu\text{m}$ ) bands with magnitude completeness limits for stars of  $I = 18^{\text{m}}5$ ,  $J = 16^{\text{m}}5$  and  $K = 14^{\text{m}}0$  leading to a prediction of the detection of 100 million stars (see <http://www-denis.iap.fr> for further details). The DENIS completeness limits (total magnitudes) for highly reliable automated galaxy extraction away from the ZOA ( $|b| > 10^\circ$ ) was determined as  $I = 16^{\text{m}}5$ ,  $J = 14^{\text{m}}8$ ,  $K_s = 12^{\text{m}}0$  by Mamon (1998), leading to a predicted extraction of roughly 250 000 galaxies. A provisional DENIS  $I$ -band catalog of galaxies with  $I \leq 14^{\text{m}}5$  for 67% of the southern sky has been released by Paturel, Rousseau & Vauglin (2003), and over 2000 serendipitous DENIS detections of galaxies behind the Milky Way by Vauglin et al. 2002 (see also Rousseau et al. 2000 for the description of some noteworthy DENIS galaxies uncovered in the ZOA). Results of pilot studies in probing the ZOA using DENIS data concentrated on the Great Attractor region, in particular in the surroundings of the cluster ACO 3627 and the radio source PKS 1343–601, have been given in Schröder et al. (1997, 1999, 2000, 2005) and Kraan-Korteweg et al. (1998), and KK&L2000.

2MASS, the 2 Micron All Sky Survey, covers the whole sky in the  $J$  ( $1.25\mu\text{m}$ ),  $H$  ( $1.65\mu\text{m}$ ) and  $K_s$  ( $2.15\mu\text{m}$ ) bands. Its point source sensitivity limits are  $J = 15^{\text{m}}8$ ,  $H = 15^{\text{m}}1$  and  $K = 14^{\text{m}}3$ , whereas for galaxies and other spatially resolved objects, the survey should be complete away from the Galactic Plane to  $J = 15^{\text{m}}0$ ,  $H = 14^{\text{m}}3$  and  $K = 13^{\text{m}}5$  over a wide range of surface brightnesses (Jarrett et al. 2000a,b). Source extraction resulted in a Point Source Catalog (PSC) containing close to half a billion objects, most of which will be Milky Way stars (next to an estimated 3 to 5 million unresolved galaxies), as well as the 2MASS Extended Source Catalog (2MASX) which contains 1.65 million galaxies or other extended sources.

In the following, we will discuss the effectiveness of 2MASX with regard to Zone of Avoidance penetration and compare this to the reduced optical ZOA including the results from the deep optical surveys. This not only to

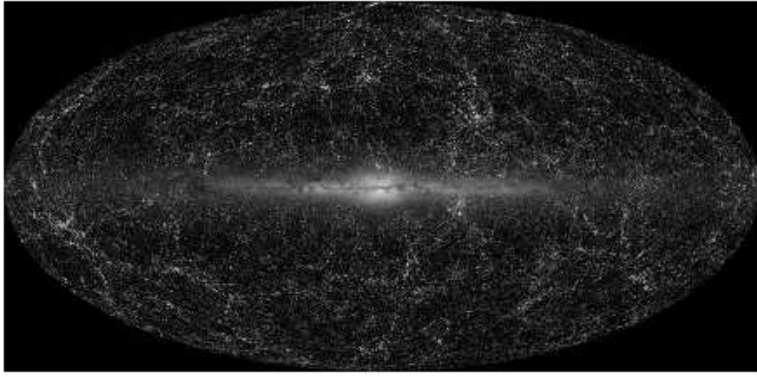


Figure 7: Distribution of 2MASX sources with  $K < 14^m0$  in an equal area Aitoff projection in Galactic coordinates centered on the Galactic Bulge. Stars from the PSC area also displayed. Figure adopted from Jarrett 2004.

determine the most effective method of uncovering galaxies hidden by the Milky Way, but by studying the magnitude completeness limits, colors and surface brightness as a function of extinction or star density, we hope, amongst others, to also optimize redshift follow-up observations in the ZOA.

### 3.1 The 2MASX Zone of Avoidance

The final release of the 2MASX by the Two Micron All Sky Survey Team in 2003 (Jarrett et al. 2000b) now allows a detailed study of the performance of 2MASS in mapping the extragalactic large-scale structures across the ZOA, as well as compare and cross-correlate the 2MASS galaxy distribution with the deep optical ZOA catalogs (see also Kraan-Korteweg & Jarrett 2005).

Fig. 7 (adopted from Jarrett 2004) shows an Aitoff projection in Galactic coordinates centered on the Galactic Bulge of all the 1.65 million resolved MASX sources with magnitudes brighter than  $K < 14^m0$ , in addition to the nearly 0.5 billion Milky Way stars. A description of the large-scale structure of these galaxies based on redshifts estimated from their NIR colors is given in Jarrett 2004. Here we will concentrate on the penetration of the ZOA.

Compared to the optical, the 2MASX sources provide a much deeper and uniform view of the whole extragalactic sky. The galaxy distribution can be traced without hardly any hindrance in the Galactic Anticenter. However, the wider Galactic Bulge region – represented here by the half billion Galactic stars from the PSC – continues to hide a non-negligible part of the extragalactic sky. Despite the fact that NIR surveys should in principle be able to uncover galaxies to extinction levels of about  $A_B = 10^m$  compared to  $3^m$  in the optical, the NIR ZOA does not appear narrower here compared to the reduced optical ZOA which on average has an approximate width of  $b \lesssim \pm 5^\circ$  around the Galactic Plane (see Fig. 4 in KK&L2000 which shows a whole-sky distribution of galaxies with  $D \geq 1/3$  that has been complemented

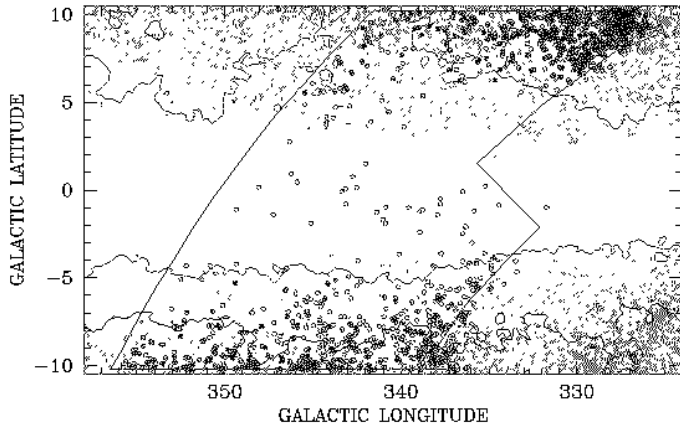


Figure 8: Distribution of optically detected galaxies (circles) with  $D > 12''$  in the Scorpius regions, and 2MASS galaxies (small dots) with  $K \leq 14^m0$  and  $(J - H) > 0^m0$  in the Scorpius search region and surroundings. The contours mark extinction levels of  $A_B = 1^m0$  and  $3^m0$ .

with all published ZOA galaxies that also meet that criterium).

Thus, there clearly also exists a NIR ZOA, but its form is quite distinct from the optical one. To understand the differences between these two ZOAs we compared in detail the results from our optical survey in the Scorpius region with 2MASX detections. The Scorpius region lies to the left of the GA region (most left search area in Fig. 3) and to the right of the Galactic Center, where confusion from the foreground Milky Way is extreme.

The optical and 2MASS galaxy distributions are displayed jointly in Fig. 8. The large circles represent optically detected galaxies in Scorpius (Fairall & Kraan-Korteweg 2000, 2005), the small dots 2MASX objects with  $K \leq 14^m0$ . It should be noted that extremely blue objects ( $(J - H) < 0^m0$ ) are excluded, as well as 2MASX sources that were rejected as likely galaxy candidates upon visual examination by Jarrett (priv. comm.). These generally are Galactic objects, such as HII regions and Planetary Nebulae, the prime contaminant at  $|b| < 2^\circ$  (optical catalogs also contain a small fraction of them). The  $1^m0$  and  $3^m0$  optical extinction contours are also drawn.

Fig. 8 confirms that even this close to the Galactic Bulge, where star densities are high, deep optical searches are fairly faithful tracers of the galaxy distribution to  $A_B \sim 3^m$ , with only a few – mostly uncertain – galaxy candidates peaking through higher dust levels. Though the extinction in the  $K$ -band is only 9% of that in the  $B$ -band, only about one-third of the optically identified galaxies in the Scorpius region have a counterpart in 2MASS. Although the 2MASX sources seem to probe deeper into the Milky Way above the Galactic Plane, this trend is not seen at negative latitudes. There, clearly optical galaxies dominate and they also probe the galaxy distribution deeper into the plane.

A direct correlation between dust absorption and 2MASX source density is not seen here. NIR surveys become progressively less successful compared to optical surveys when approaching the Galactic Center. In fact, this progressive loss of 2MASX galaxies is already noticeable in the fraction of optical galaxies that have counterparts in the 2MASX catalog. This fraction is 47% in the Hydra/Antlia region ( $\ell \approx 280^\circ$ ; see Fig. 3 for orientation), and decreases to 39% in the Crux region ( $\ell \approx 310^\circ$ ), 37% in the GA region ( $\ell \approx 325^\circ$ ), 33% in the Scorpius region ( $\ell \approx 340^\circ$ ), and to a mere 16% in the by Wakamatsu et al. (2000, 2005) explored Ophiuchus cluster region ( $\ell = 0^\circ.5, b = +9^\circ.5$ ).

It should be maintained though, that there also are 2MASX galaxies in the optically surveyed regions that have no optical counterpart. This fraction increases inversely, i.e. the farther away from the Galactic Bulge the higher this fraction. Not unsurprisingly, the majority of ZOA galaxies that are seen in 2MASS galaxies but not in the optical are on average quite red and faint (mostly with  $K \gtrsim 12^m$ ). This is partly a ZOA effect with NIR surveys finding red galaxies more readily at higher absorption level. But it is also due to the inherent characteristics of the two surveys. Whereas the NIR is better at detecting old galaxies and ellipticals, the optical surveys – although susceptible to all galaxy types – are best at finding spirals and late-type galaxies (especially low surface-brightness galaxies and dwarfs). The surveys are in fact complementary.

The success rate of galaxy identification in the NIR actually depends much more strongly on *star density* than dust extinction. This effect is corroborated by Fig. 9, which shows 2MASX sources with  $K \leq 14^m.0$  within  $\pm 15^\circ$  of the Galactic equator. In the left panel, DIRBE/IRAS extinction contours of  $A_B = 1^m.0, 3^m.0$  and  $5^m.0$  are superimposed. The right panel emphasizes the locations of 2MASX sources in regions where the density of stars in the PSC with  $K \leq 14^m.0$  per square degree is  $\log N = 3.50, 3.75$ , and  $4.00$ .

An examination of the dust extinction contours with the area in which 2MASX does not find extended sources does not suggest a correlation between them. In the Galactic Anticenter, roughly defined here as  $\ell \sim 180^\circ \pm 90^\circ$ , 2MASX objects seem to cross the Plane without any hindrance. For this half of the ZOA, plots of NIR magnitude or diameter versus extinction (not shown here) confirm that galaxies can be easily identified up to extinction levels equivalent to  $A_B \gtrsim 10^m$ , and extinction-corrected  $K^o$ -band magnitudes versus extinction diagrams imply that 2MASS remains quite complete up to  $K^o \lesssim 13^m.0$  for  $A_B \sim 10^m.5$ .

This is not at all true for the wider Galactic Bulge region ( $\ell \sim 0^\circ \pm 90^\circ$ ), where 2MASX detects objects to lower extinction levels only and where the completeness limit is at least one magnitude lower compared to the Anticenter. And although Galactic dust does reduce the completeness limit of 2MASX sources at low latitudes – although to a much lower extent than in the optical – the origin of the NIR ZOA is mainly due to source confusion in regions of high *star density*.

This region in which NIR surveys fail completely has a very well-defined shape. It is traced by the star density isopleth (stars per square degree with

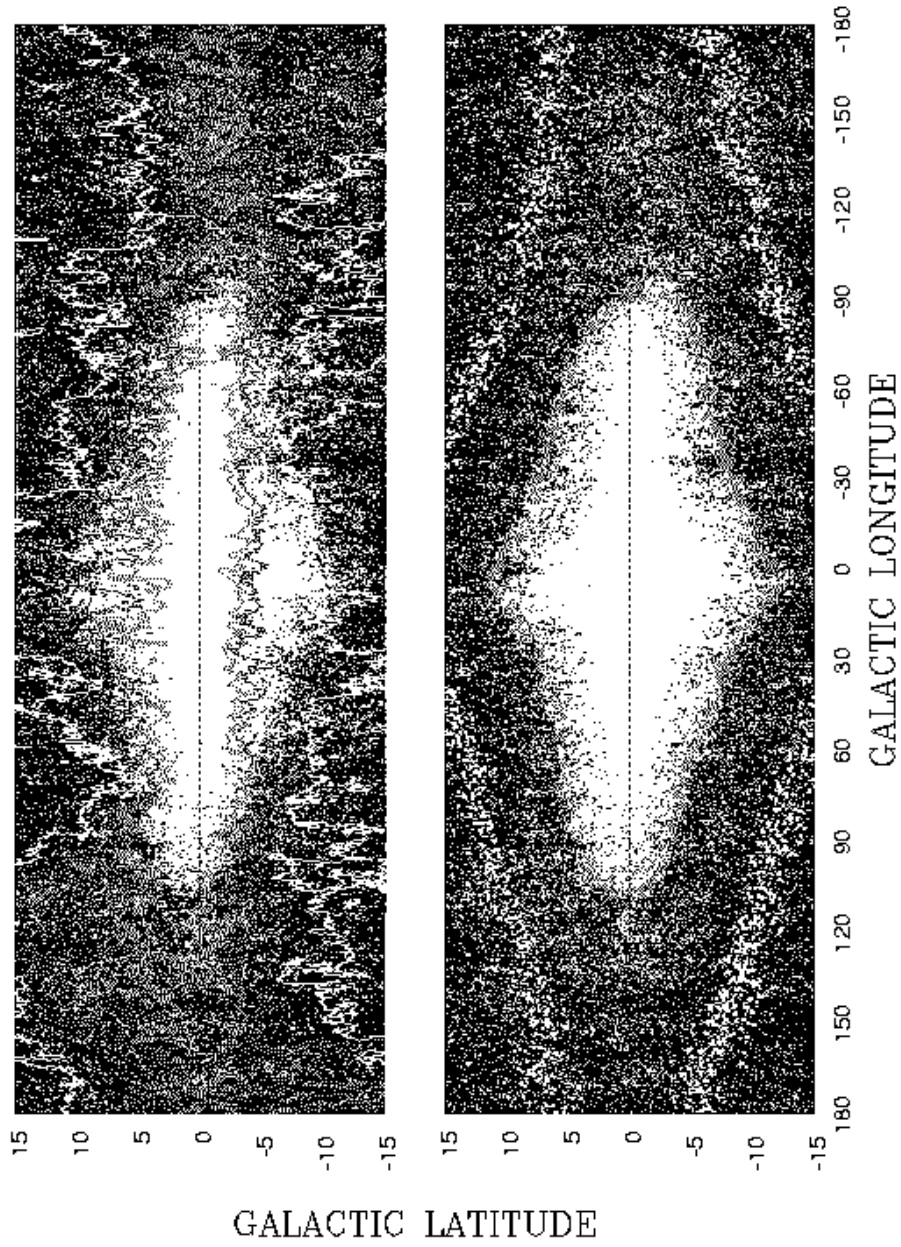


Figure 9: Distribution of 2MASX sources with  $K \leq 14^m0$  along the Galactic equator within  $b \leq \pm 15^\circ$ . In the left panel, DIRBE/IRAS extinction contours of  $A_B = 1^m0, 3^m0$  and  $5^m0$  are superimposed. In the right panel, galaxies found in regions of star densities of  $\log N = 3.50, 3.75$ , and  $4.00$  per square degree ( $K \leq 14^m0$ ) are enhanced.

$K < 14^m0$ ) of  $\log(N) = 4.00$ , i.e. the innermost contour in the right panel of Fig. 9. At this level, the completeness has already dropped significantly. Above this limit, the point sources are packed so densely that extended sources can not be extracted anymore. The hoped-for improvement of uncovering the galaxy overdensity with NIR surveys to lower latitudes compared to the optical, as for instance in the Great Attractor region (compare Fig. 3 or 5 to Fig. 7), has not been achieved.

It should be maintained, however, that for the ZOA away from the Bulge – as well as for the rest of the sky – 2MASS as a homogeneous whole-sky survey obviously is far superior. An optimal approach in revealing the galaxy distribution behind the Milky Way will actually result from a combination of deep optical and near-infrared surveys. Not only because of the different susceptibility to morphology, but because the former are sensitive to galaxies located behind regions of high source confusion, and the latter to galaxies located behind thick dust walls.

A reduction of the ZOA common to both the optical and NIR might be achieved by a combination of a deep  $R$ -band survey with a spatially higher resolved NIR survey (higher than the current NIR surveys 2MASS and DENIS) which should diminish the source confusion in high star density regions.

### 3.2 The Shape of the NIR ZOA

For the discussion in this section on the shape of the NIR ZOA, we define it more or less ad hoc as the nearly completely empty region as outlined by the isopleth given with the 2MASS PSC star density of  $\log N = 4.00$  per square degree for stars with  $K \leq 14^m0$  (inner contour of left panel of Fig. 9). A closer look at the NIR ZOA reveals some interesting asymmetries that are independent of extragalactic large-scale structure but are actually due to Galactic structure.

The bulge and disk as outlined by the lack of galaxies seem to be inclined with respect to the Galactic equator. Its mean latitude is offset to positive latitudes for  $\ell \sim 90^\circ$ , and to negative latitudes for  $\ell \sim 270^\circ$  ( $-90^\circ$ ). This lopsidedness has been known for a long time. It was first established from the Galactic hydrogen column densities by Kerr & Westerhout in 1965 for longitudes between  $\ell = 220^\circ - 330^\circ$ . The same inclination is evidenced also in the dust contours (see left panel of Fig. 9).

Another asymmetry becomes obvious when regarding the width of the NIR ZOA with respect to the Galactic Center. Whereas the NIR ZOA can be followed to about  $\ell \sim 120^\circ$  on the one side, it stretches over 'only'  $90^\circ$  on the opposite side of the Galactic Center (to  $\ell \sim 270^\circ$ ). The explanation for this asymmetry lies in the relative location of the Sun with respect to the Galactic spiral arms. When looking towards the local Orion arm, our line of sight is hit directly with a high density of nearby stars, blocking a larger fraction of the extragalactic sky from our view, whereas the opposite line of sight is nearly free of stars for quite a distance until it hits the more distant spiral arm, allowing us to identify galaxies more easily between the fainter



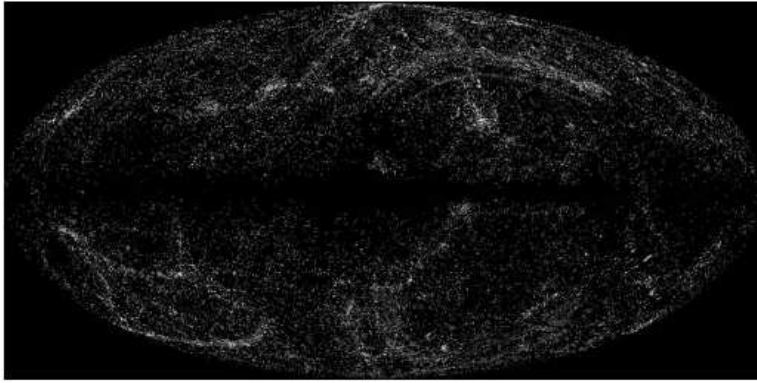


Figure 10: Distribution of 2MASX sources in an equal area Aitoff projection in Galactic coordinates that have redshifts listed in NED (Jarrett 2004, priv. comm.).

and smaller stars of this star population.

Furthermore, when regarding the location where the Galactic Bulge is highest, one notes that it does not peak at  $\ell = 0^\circ$  as expected, but is centered on  $\ell \sim +5^\circ$ . This offset probably is due to the bar of our Galaxy. Its near side points towards us (positive longitudes), reducing our view of the extragalactic sky stronger compared to our line of sight towards the far side of the Galactic bar.

As these asymmetries have more to do with Galactic structure than extragalactic structure, one might be tempted to ignore them. However, these asymmetries in the distribution of galaxies should be taken into account when using the 2MASX catalog – or redshift surveys based on 2MASX subsamples – for dipole determinations. These structures might have a significant effect on the results if not properly corrected for.

### 3.3 A Redshift Zone of Avoidance

A reduction of the ZOA on the sky does not imply at all that a similar reduction can also be attained in redshift space. This is seen most clearly in Fig. 10 which displays the distribution of 2MASX galaxies that have a redshift listed in NED, the NASA/IPAC Extragalactic Database (Jarrett 2004, priv. comm.). The ZOA in this figure is quite distinct from the previously defined NIR ZOA. Its form is actually much more reminiscent of the optical ZOA delimited by the extinction contour of  $A_B = 3^m0$  (see Fig. 4 in KK&L2000). Hardly any redshifts are available for latitudes of  $b \lesssim 5^\circ$ .

One might argue that this is an artifact because it is based mainly on optically selected targets. 2MASX has been released only fairly recently and systematic follow-up redshifts observations of the newly uncovered galaxies at low Galactic latitudes, in particular in the Galactic Anticenter ZOA half, have

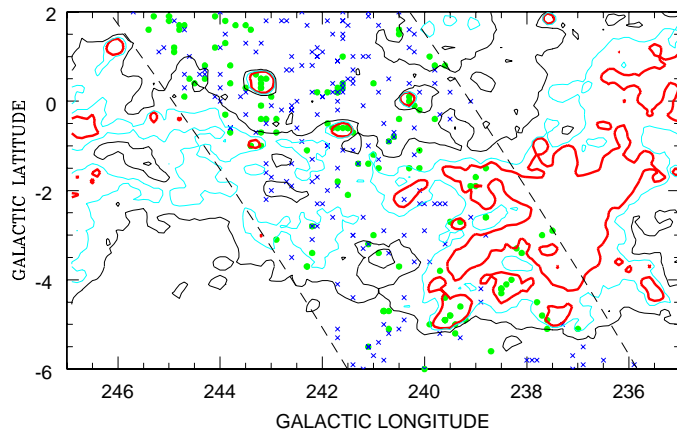


Figure 11: Distribution of 2MASS galaxies observed with 6dF in a strip crossing the Galactic Plane in the Puppis region. Circles represent galaxies with redshifts, crosses those without a reliable redshift determination. The contours indicate an optical extinction of  $A_B = 1^m0, 2^m0$  and  $3^m0$  (thick contour).

not yet been made and/or published. This is however not entirely true. In whatever kind of waveband a ZOA galaxy is identified, it remains inherently difficult to obtain a reliable optical redshift when the extinction in the optical towards this galaxy exceeds 3 magnitudes, i.e. the delimiting factor of optical surveys in general.

This is seen quite clearly in Fig. 11 which shows 2MASS galaxies in Puppis – a filament is crossing the Plane there (see Fig. 7) – on a sequence of 6-degree fields (6dF) centered on  $\text{Dec} = -25^\circ$ . This strip has been observed with the multifibre spectroscope at the UK Schmidt Telescope as part of a pilot project aimed at extending the 6dF Galaxy Survey towards lower latitudes. It now is restricted to the southern sky with  $|b| \geq 10^\circ$  (see <http://www.mso.anu.edu.au/6dFGS> for further details).

The crosses mark galaxies for which a reliable redshift could be measured, the filled dots galaxies for which this could not be realized. At first glance, the plot seems to indicate a fantastic success rate for obtaining redshifts all the way across the Milky Way. However, it should be noted that the concerned ZOA strip lies in a region renowned for its low dust content (it hardly exceeds 3 magnitudes), and a careful inspection indicates that redshifts have generally not been obtained for galaxies that lie in pockets where the extinction is higher than  $A_B \gtrsim 3^m0$  (thick contour). So even when galaxies are identifiable deep in the Plane, reducing the *redshift* ZOA will remain hard, and an optimization of targeted ZOA galaxies is crucial for redshift follow-ups.

## 4 Dedicated HI Galaxy Searches in the ZOA

Because the Galaxy is fully transparent to the 21cm line radiation of neutral hydrogen, HI-rich galaxies can readily be found through the detection of their redshifted 21cm emission in the regions of the highest obscuration and infrared confusion. Furthermore, with the detection of an HI signal, the redshift and rotational properties of an external galaxy are immediately known, providing insight not only on its location in redshift space but also on the intrinsic properties of such obscured galaxies. This makes systematic blind HI surveys powerful tools in mapping large-scale structures behind the Milky Way.

Early-type galaxies – tracers of massive groups and clusters – are gas-poor and will, however, not be identified in these surveys. Furthermore, low-velocity extragalactic sources that fall within the velocity range of the strong emission of the Galactic gas ( $v \lesssim \pm 250 \text{ km s}^{-1}$ ) will be missed. Galaxies that lie close in position to radio continuum sources may also be missed because of the baseline ripples they produce over the whole observed frequency range.

Two systematic blind HI searches for galaxies behind the Milky Way have been made. The first used the 25 m Dwingeloo radio to survey the whole northern Galactic Plane for galaxies out to  $4000 \text{ km s}^{-1}$  with a sensitivity of *rms* of 40 mJy for a 1 hr integration (see KK&L2000 for a summary of the results). A more sensitive survey (*rms* of typically 6 mJy beam $^{-1}$ ), probing a considerably larger volume (out to  $12\,700 \text{ km s}^{-1}$ ), has been performed with the Multibeam Receiver at the Parkes 64m radio telescope in the southern sky. In the following, the most recent results of this survey are given.

### 4.1 The Parkes Multibeam HI ZOA Survey

The Multibeam receiver at the 64m Parkes telescope was specifically constructed to efficiently search for galaxies of low optical surface brightness, or galaxies at high optical extinction, over large areas of the sky. It has 13 beams, each with a beamwidth of  $14'4$ , arranged in a hexagonal grid in the focal plane array (Staveley-Smith et al. 1996) which allows – with its large footprint of  $2^\circ5$  on the sky – rapid sampling of large areas.

In March 1997, this instrument was mounted on the telescope and various surveys were started, one being a systematic blind HI survey within  $b < \pm 5^\circ$  of the ZOA. The observations were performed in scanning mode. Fields of length  $\Delta\ell = 8^\circ$  centered on the Galactic Plane were surveyed along constant Galactic latitudes where each scan was offset by  $35'$  in latitude until the final width of  $\Delta b = \pm 5^\circ$  had been attained (17 passages back and forth). The final goal was 25 repetitions per field. With an effective integration time of 25 min/beam, a  $3\sigma$  detection limit of 25 mJy was obtained. The correlator bandwidth of 64 MHz was set to cover a velocity range of  $-1200 \lesssim v \lesssim 12700 \text{ km s}^{-1}$ . The survey therewith is sensitive to normal spiral galaxies well beyond the Great Attractor region (e.g.  $5 \cdot 10^9 M_\odot$  at 60 Mpc for a galaxy with a linewidth of  $200 \text{ km s}^{-1}$ ), next to the lowest mass dwarf galaxies in the local neighborhood ( $10^6 - 10^7 M_\odot$ ), or extremely massive galaxies beyond  $10\,000 \text{ km s}^{-1}$  such as

the extraordinarily massive galaxy HIZOA J0836-43 with a HI mass of  $7 \cdot 10^{10} M_{\odot}$  found in one of the ZOA data cubes (Kraan-Korteweg et al. 2005b; Donley et al. in prep.).

The data are in the form of three-dimensional data cubes (position-position-velocity, with pixel and beam sizes of  $4' \times 4'$ , and  $15'5$ , respectively). Experimentation with automatic galaxy detection algorithms indicated that visual inspection of the data cubes is more efficient for the ZOA, where the noise due to continuum sources and Galactic HI is high and variable. The ZOA cubes were inspected by at least two, sometimes three, individual researchers, with the subsequent neutral evaluation of inconsistent cases in the detection lists by a third party.

An first analysis covering the *southern* Milky Way ( $212^{\circ} \leq \ell \leq 36^{\circ}$ ) based on 2 out of the foreseen 25 passages (the HI ZOA Shallow Survey; henceforth HIZSS) with and *rms* noise of  $13 \text{ mJy beam}^{-1}$  led to the discovery of 110 galaxies, two thirds of which were previously unknown (Henning et al. 2000). A final catalog of the 23 central cubes of the full-sensitivity survey is in preparation (Henning et al., in prep.).

The data and plots of the full sensitivity survey are presented in the next section. They are based on a provisional version of this catalog which might still contain a few galaxy candidates that will be rejected for inclusion in the final catalog. They furthermore include detections from an extension to the north ( $\text{Dec} > 0^{\circ}$ ), which was done at a later stage, resulting in 2 further cubes on both sides of the southern ZOA (Donley et al. 2005). The data set regarded here thus consists of 27 data cubes that cover the ZOA between  $196^{\circ} \leq \ell \leq 52^{\circ}$  for  $|b| \leq 5^{\circ}$ . A total of slightly over one thousand galaxies were identified in these data cubes.

## 4.2 The Detected Galaxies

Figure 12 displays the distribution along the Milky Way of the in HI detected galaxies. An inspection of this distribution shows that the HI survey nearly fully penetrates the ZOA with hardly any dependence on Galactic latitude.

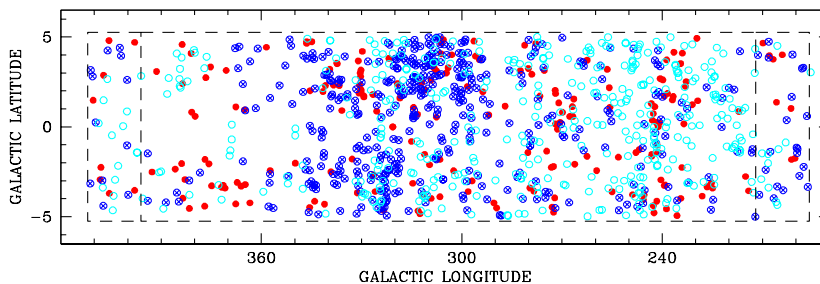


Figure 12: Distribution in Galactic coordinates of the galaxies detected in the deep HI ZOA survey. Open circles:  $v_{\text{hel}} < 3500$ ; circled crosses:  $3500 < v_{\text{hel}} < 6500$ ; filled circles:  $v_{\text{hel}} > 9500 \text{ km s}^{-1}$ .

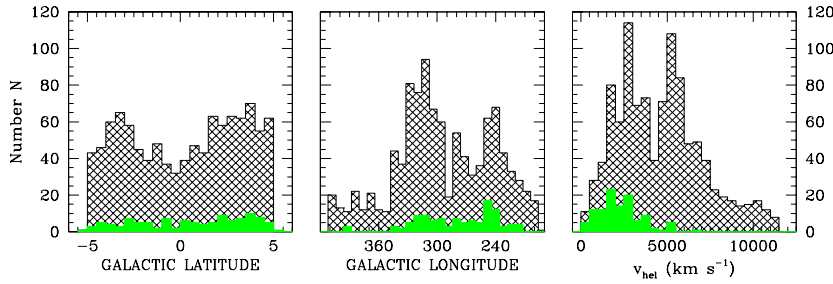


Figure 13: Distributions as a function of the Galactic latitude, longitude and the heliocentric velocity of the in HI detected galaxies. The lower histograms represent the results from the HIZSS.

This is confirmed by the left panel in Fig. 13, which shows the detection rate as a function of Galactic latitude. The small dip in the detection rate between  $-2^\circ \lesssim b \lesssim +1^\circ$  stems mainly from the Galactic Bulge region and to a lesser extent from the GA region ( $\ell \approx 300^\circ - 340^\circ$ ). The former is due to the high number of continuum sources at low latitudes in the Galactic Bulge region. In the GA region the gap is possibly related to the high galaxian density for the on average higher velocity, hence fainter, galaxies. There, a moderate number of continuum sources may already result in a detection-loss. This explanation is supported by the fact that this dip is not noticeable in the shallower HIZSS data (lower histogram).

A much stronger variation is apparent in the number density as a function of Galactic longitude (see also middle panel of Fig. 13). This can be explained entirely with large-scale structures such as the nearby (and therefore prominent in HIZSS) Puppis filament ( $\ell \approx 240^\circ$ ), the Hydra-Antlia filament ( $\ell \approx 280^\circ$ ), the very dense GA region ( $\ell \approx 300 - 340^\circ$ ), followed by an under-dense region ( $52^\circ \gtrsim \ell \gtrsim 350^\circ$ ) due to the Local and Sagittarius Void.

These large-scale structures have left their imprint also on the velocity diagram (right panel of Fig. 13), which shows two conspicuous broad peaks. The low-velocity one is due to a blend of various structures in or crossing the Galactic Plane while the second around  $5000 \text{ km s}^{-1}$  clearly is due to the GA overdensity (see also Fig. 14 – 16). The velocity histogram moreover shows that galaxies are found all the way out to the velocity limit of the survey of  $\sim 12000 \text{ km s}^{-1}$ , hence probe the galaxy distribution considerably deeper than either the shallow ZOA survey HIZSS (lower histogram), or the southern sky HI surveys also made with the Multibeam instrument, the HI Bright Galaxy Catalog (BGC; Koribalski et al. 2003) and the HI Parkes All Sky Survey (HIPASS; Meyer et al. 2004).

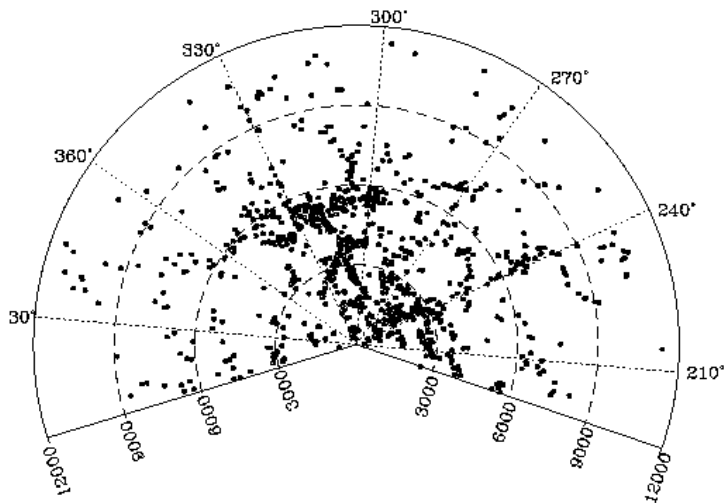


Figure 14: Galactic latitude slice with  $|b| \leq 5^\circ$  out to  $12000 \text{ km s}^{-1}$  of the slightly over 1000 in HI detected galaxies. Circles mark intervals of  $3000 \text{ km s}^{-1}$ .

### 4.3 Uncovered Large-Scale Structures in the GA

Figure 14 shows a Galactic latitude slice with  $|b| \leq 5^\circ$  out to  $12000 \text{ km s}^{-1}$  of the galaxies detected in the deep Parkes HI ZOA survey (henceforth HIZOA) for the longitude range  $196^\circ \leq \ell \leq 52^\circ$ . The clear conclusion when inspecting this figure is that the HI survey really permits the tracing of large-scale structures in the most opaque part of the ZOA; and this in a homogenous way, unbiased by the clumpiness of the foreground dust contamination.

In the following, some of the most interesting features revealed in Fig. 14 will be discussed. It is suggested to simultaneously consult Fig. 15, which shows the HIZOA data with data extracted from LEDA surrounding the ZOA in sky projections for three velocity shells of thickness  $3000 \text{ km s}^{-1}$ . This helps to show the newly discovered features in context to known structures. Viewing the distribution of galaxies within  $\Delta b \leq 5^\circ$  in this figure illustrates quite clearly how the HI survey has managed to fill in that part of the ZOA, tracing various contiguous structures across the plane of the Milky Way.

The most prominent large-scale structure in Fig. 14 certainly is the Norma Supercluster which seems to stretch from  $360^\circ$  to  $290^\circ$  in this plot, lying always just below the  $6000 \text{ km s}^{-1}$  circle, with a weakly visible extension towards Vela ( $\sim 270^\circ$ ). The latter is more pronounced at higher latitudes (see panel 2 in Fig. 15, and Fig. 16). This wall-like feature seems to be formed of various agglomerations. The first one around  $340^\circ$  is seen for the first time with new HI data. Because of the high extinction there, it cannot be assessed whether this overdensity continues for  $|b| > 5^\circ$ . The clump at  $325^\circ$  is due to the outer boundaries at lower latitudes side of the Norma cluster A3627

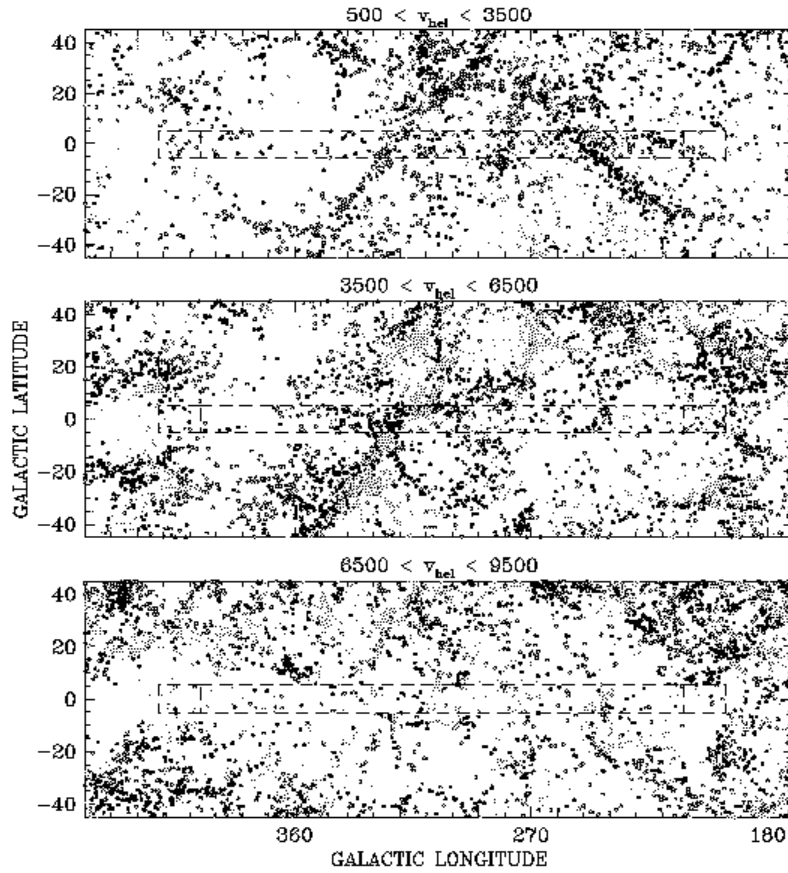


Figure 15: Sky projections of three redshift slices of depth  $\Delta v = 3000 \text{ km s}^{-1}$  showing the HIZOA data in combination with data from LEDA. The HIZOA survey area is outlined.

( $\ell, b, v = 325^\circ, -7^\circ, 4880 \text{ km s}^{-1}$ ; Kraan-Korteweg et al. 1996). The next two are previously unrecognized due to groups (or small clusters) at  $310^\circ$  and  $300^\circ$ , both at  $|b| \sim +4^\circ$ . They are very distinct in the middle panel of Fig. 15. Between these two clusters at slightly higher latitude we see a small finger of God, which belongs to the Centaurus-Crux/CIZA J1324.7–5736 cluster.

This is not the only overdensity in the GA region. A significant agglomeration of galaxies is evident closer by at  $(\ell, v) = (311^\circ, 3900 \text{ km s}^{-1})$  with two filaments merging into it. Although no finger of God is visible (never very notable in HI redshift slices), this concentration forms part of the previously discussed galaxy concentration around the strong radio source PKS 1343–601 which is consistent with an intermediate size cluster residing there.

Next to the Norma cluster, only the Centaurus-Crux cluster has an appreciable X-ray emission (Ebeling et al. 2002; Mullis et al. 2005). It seems

therefore unlikely that any of the newly apparent galaxy concentrations are a signature of a further massive cluster that conforms part of the GA overdensity. But it should be kept in mind that X-ray photons are subjected to photoelectric absorption by the Galactic hydrogen atoms – the X-ray absorbing equivalent hydrogen column density – which does limit detections close to the Galactic Plane. This effect is particularly severe for the softest X-ray emission, as observed by ROSAT (0.1-2.4 keV), and is seen in the CIZA cluster distribution (CIZA standing for Clusters in the Zone of Avoidance, a systematic search for X-ray clusters with Galactic latitudes  $|b| \leq 20^\circ$ ). Hardly any clusters are found for Galactic HI column density over  $N_{\text{HI}} > 5 \times 10^{21} \text{ cm}^{-2}$ , which creates an X-ray ZOA of about  $\Delta b \lesssim 5^\circ$  on average (see Fig. 14 in KK&L2000; Fig. 7 in Ebeling et al. 2002).

Although the overdensity in the GA region looks quite impressive here, a preliminary quantitative analysis of the 4 cubes covering  $300^\circ \leq \ell \leq 332^\circ$  by Staveley-Smith et al. (2000) find a mass excess of 'only'  $\sim 2 \cdot 10^{15} \Omega_0 M_\odot$  over the background, thus considerably lower than the predictions from the infall pattern. Then again, the signatures of overdensities and clusters are overall much shallower in HI surveys compared to, e.g., optical surveys (e.g. Fig. 22 versus Fig. 23 in Koribalski et al. 2004).

To the left of the GA overdensity a few other features are worthwhile describing. An underdense region comprised of the Local Void and the Sagittarius Void is seen around  $\ell = 360^\circ$  at central velocities of  $\sim 1500$  and  $4500 \text{ km s}^{-1}$  (see also the first two panels of Fig. 15). Except for the tiny group of galaxies at about  $(350^\circ, 3000 \text{ km s}^{-1})$ , the distribution here and in Fig. 14 suggest one big void rather than two separate ones. In contrast, the righthand side of Fig. 15 is quite crowded: the Puppis region ( $\ell \sim 240^\circ$ ) with its two nearby groups ( $800$  and  $1500 \text{ km s}^{-1}$ ) followed by the Hydra Wall at about  $3000 \text{ km s}^{-1}$  that extends from the Monoceros group ( $210^\circ$ ) to the concentration at  $280^\circ$ . The latter is not the signature of a group but due to a filament emerging out of the Antlia cluster ( $273^\circ, 19^\circ$ ; see Fig. 15).

With this systematic HI survey, we could map for the first time large-scale structures without any hindrance across the Milky Way (Figs. 14 and 15). It is the only approach that easily uncovers galaxies in the ZOA - and records their redshift. For this reason we are currently extending the Parkes HI ZOA survey to higher Galactic latitudes in the Galactic Bulge region ( $332^\circ < \ell < 36^\circ$ ) where the optical and NIR ZOAs are wider and knowledge about the structures very poor. They will improve the knowledge on the borders of the Local and Sagittarius Void, as well as the Ophiuchus cluster studied optically by Wakamatsu et al. (2000; 2005).

## 5 Discussion

In the last decade, enormous progress has been made in unveiling the extragalactic sky behind the Milky Way. At optical wavebands, the entire ZOA has been systematically surveyed, reducing the optical ZOA by about a factor



of  $2 - 2.5$ , i.e. from  $A_B = 1^m0$  to  $A_B = 3^m0$ . Its average width is about  $\pm 5^\circ$ , except in the low-extinction Puppis area, where galaxies have been found at all latitudes, in contrast to the Galactic Bulge region where the  $3^m0$  contour rises to higher latitudes for positive latitudes.

2MASS, as a homogeneous NIR survey, obviously is far superior to optical surveys, particularly considering that the optical ZOA surveys were not only performed on different plate material, but also by different searchers using different search techniques. Nevertheless, in the regions of highest star densities (over 10 000 stars with  $K \leq 14^m$  per square degree), i.e. around the Galactic Bulge ( $\ell \lesssim \pm 90^\circ$ ), the identification of galaxies fails for latitudes between  $\pm 5^\circ$  up to  $\pm 10^\circ$  (see innermost contour in right panel of Fig. 9) and the hoped-for improvement of uncovering further galaxy overdensities in, for instance, the Great Attractor, could not be realized.

Even when a galaxy can be identified at high extinction levels, such as is possible in the NIR and FIR, this will, however, not automatically reduce the ZOA in redshift space. As discussed in Sect. 3.3 (see Fig. 10) it remains nearly impossible to obtain optical redshifts for galaxies at extinction levels  $A_B \gtrsim 3^m$ . At these levels only HI observations prevail – if the galaxies are gas-rich and not too distant. But even with a HI detection, cross-identification with its optical, 2MASS and/or IRAS counterpart (Donley et al. 2005) often remains ambiguous because of positional uncertainty due to the large beams of single-dish radio telescopes.

As seen in this paper, the mapping of the galaxy distribution behind the Milky Way requires considerable efforts. Still, combining data obtained from the various multi-wavelength approaches will reveal this hidden part of the Universe, as clearly illustrated with Fig. 16 for the Great Attractor region – though a quantification of the structures will remain difficult due to the different biases and selection effects in the different methods.

Figure 16 shows a redshift slice of width  $|b| \leq 10^\circ$  out to  $12\,000\text{ km s}^{-1}$  compared to the  $\pm 5^\circ$  of the HI data alone. All galaxies with a redshift in the LEDA data base are included next to the data from the HIZOA. Note that this is not a homogenous data set. It clearly is deeper sampled from  $270^\circ \lesssim \ell \lesssim 340^\circ$  because of the intensive redshift follow-up programs of the ZOA catalogs by Kraan-Korteweg, Woudt and collaborators in that longitude range (see Sect. 2.1).

Before the ZOA research programs, this slice only had a few points in them – mainly in the low extinction Puppis area ( $\ell \sim 240^\circ$ ) – and certainly did not allow any reliable description of large-scale structures. It now has been filled to a depth comparable to unobscured regions in the sky and the above diagram reveals various clusters, filamentary and wall-like structures, next to some sharply outlined voids which finally allow a fairly profound glimpse at the previously hidden core of the Great Attractor. Fig. 16 clearly shows the prominence of the Norma cluster ( $\ell = 325^\circ$ ) as well as its central location in the great-wall like structure that can be followed from  $270^\circ$  to  $360^\circ$  within the redshift range  $4000 - 6000\text{ km s}^{-1}$ . In front of this wall, we see further filaments that merge in the galaxy concentration around PKS 1343–601. The combined

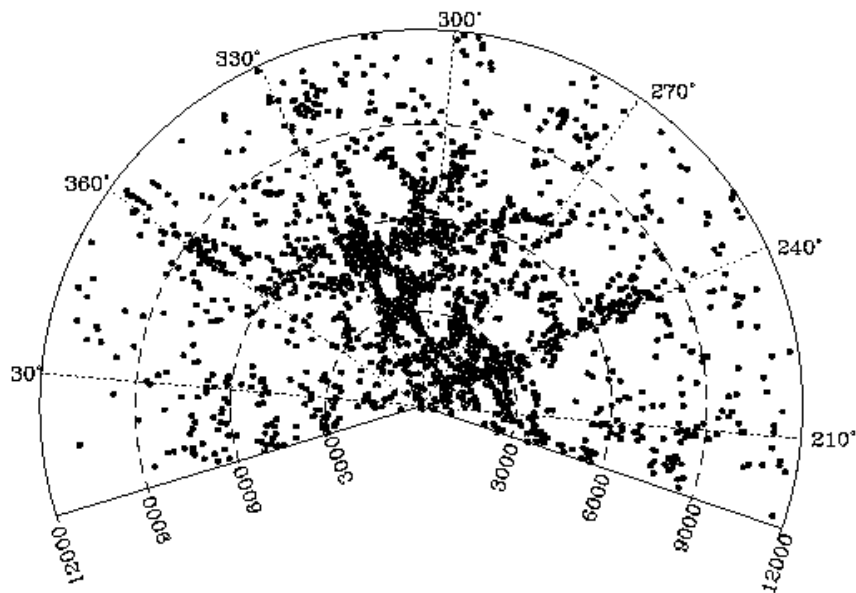


Figure 16: Galactic latitude slice within  $|b| \leq 10^\circ$  out to  $12000 \text{ km s}^{-1}$  with all the galaxies extracted from LEDA, including the HI Multibeam data displayed in Fig. 14.

structures in the vicinity of the Norma cluster show a strong similarity to the Coma cluster in the Great Wall from the CfA redshift slices by Huchra, Geller and collaborators. The flow field that pointed to a so-called Great Attractor does seem explained by what we now call the Norma Supercluster, together with the galaxy concentration around PKS 1343–601, as well as the Centaurus Wall, that stretches from the Pavo cluster ( $332^\circ, -23^\circ$ ) across the Galactic Plane to the Centaurus cluster ( $320^\circ, +22^\circ$ ) at slightly lower velocities than the Norma Supercluster.

## Acknowledgements

Discussions with P.A. Woudt and T. Jarrett have been invaluable in the preparation of this review. The contributions of the ZOA team L. Staveley-Smith (PI), B. Koribalski, P.A. Henning, A.J. Green, R.D. Ekers, R.F. Haynes, R.M. Price, E.M. Sadler, I. Stewart and A. Schröder and other participants in the Multibeam HI survey are gratefully acknowledged. This research used the Lyon-Meudon Extragalactic Database (LED A), supplied by the LED A team at the Centre de Recherche Astronomique de Lyon, Obs. de Lyon, and also the NASA/IPAC Infrared Science Archive (2MASS) and the NASA/IPAC Extragalactic Database (NED), which are operated by the Jet Propulsion

Laboratory, California Institute of Technology, under contract with the National Aeronautics and Space Administration. RCKK thanks CONACyT for their support (research grant 40094F) and the Australian Telescope National Facility (CSIRO) for their support and hospitality during her sabbatical.

## References

- Abell, G.O., Corwin, H.G.Jr., & Olowin, R.P. 1989, ApJS 70, 1
- Balkowski, C., & Kraan-Korteweg, R.C. (eds.) 1994, “Unveiling Large-Scale Structures behind the Milky Way”, ASP Conf. Ser. 67, (San Francisco: ASP)
- Böhringer, H., Neumann, D.M., Schindler, S., & Kraan-Korteweg R.C. 1996, ApJ 467, 168
- Cameron, L.M. 1990, A&A 233, 16
- Donley, J.L., Staveley-Smith, L., Kraan-Korteweg, R.C., et al. 2005, AJ 129, 220
- Dressler, A., Faber, S.M., Burstein, D., et al. 1987, ApJ 313, 37
- Ebeling, H., Mullis, C.R., & Tully, B.R. 2002, ApJ 580, 774
- Fairall, A.P., & Kraan-Korteweg, R.C. 2000, in “Mapping the Hidden Universe: The Universe behind the Milky Way - The Universe in HI”, ASP Conf. Ser. 218, eds. R.C. Kraan-Korteweg, P.A. Henning & H. Andernach, (San Francisco: ASP), 35
- Fairall, A.P., & Kraan-Korteweg, R.C. 2005, in prep.
- Fairall, A.P., & Woudt, P.A. (eds.) 2005, in “Nearby Large-Scale Structures and the Zone of Avoidance”, ASP Conf. Ser. 329 (San Francisco: ASP)
- Fairall, A.P., Woudt, P.A., & Kraan-Korteweg, R.C. 1998, A&ASS 127, 463
- Henning, P.A., Staveley-Smith, L., Ekers, R.D., et al. 2000, AJ 119, 2686
- Hudson, M.J., & Lynden-Bell, D. 1991, MNRAS 252, 219
- Hudson, M.J., Smith, R.J., Lucey, J.R., & Branchini, E. 2004, MNRAS 352, 61
- De Lapparent, V., Geller, M.J., & Huchra, J.P. 1986, ApJ 302, L1
- Jarrett, T. 2004, PASA 21, 396
- Jarrett, T.-H., Chester, T., Cutri, R., Schneider, S., Rosenberg, J., Huchra, J.P., & Mader, J. 2000a, AJ 120, 298
- Jarrett, T.-H., Chester, T., Cutri, R., Schneider, S., Skrutskie, M., & Huchra, J.P. 2000b, AJ 119, 2498
- Joint IRAS Science Working Group 1988, *IRAS Point Source Catalog*, Version 2 (Washington: US Govt. Printing Office)
- Kerr, F.J., & Westerhout, G. 1965, *Galactic Structure* (Chicago: University of Chicago), 186
- Kocevski, D.D., Mullis, C.R., & Ebeling, H. 2004, ApJ 608, 721
- Kogut, A., Lineweaver, C., Smoot, G.F., et al. 1993, ApJ 419, 1
- Kolatt, T., Dekel, A., & Lahav, O. 1995, MNRAS 275, 797
- Koribalski, B.S., Staveley-Smith, L., Kilborn, V.A., et al. 2004, AJ 128, 16

- Kraan-Korteweg, R.C. 2000, A&ASS 141, 123
- Kraan-Korteweg, R.C., & Jarrett, T. 2005, in “Nearby large-Scale Structures and the Zone of Avoidance”, ASP Conf. Ser. 329, eds. A.P. Fairall & P.A. Woudt, (San Francisco: ASP), 119 (astro-ph/0409391)
- Kraan-Korteweg, R.C., & Lahav, O. 2000, A&ARv 10, 211
- Kraan-Korteweg, R.C., & Woudt, P.A. 1999, PASA 16, 53
- Kraan-Korteweg, R.C., Loan, A.J., Burton, W.B., Lahav, O., Ferguson, H.C., Henning, P.A., & Lynden-Bell, D. 1994, Nature 372, 77
- Kraan-Korteweg, R.C., Fairall, A.P., & Balkowski, C. 1995, A&A 297, 617
- Kraan-Korteweg, R.C., Woudt, P.A., Cayatte, V., Fairall, A.P., Balkowski, C., & Henning, P.A. 1996, Nature 379, 519
- Kraan-Korteweg, R.C., Schröder, A., Mamon, G., & Ruphy S. 1998, in “The Impact of Near-Infrared Surveys on Galactic and Extragalactic Astronomy”, ed. N. Epchtein (Kluwer: Dordrecht), 205
- Kraan-Korteweg R.C., Henning P.A., & Andernach H. (eds.) 2000, in “Mapping the Hidden Universe: The Universe Behind the Milky Way – The Universe in HI”, ASP Conf. Ser. 218 (San Francisco: ASP)
- Kraan-Korteweg R.C., Henning P.A., & Schröder, A.C. 2002, A&A 391, 887
- Kraan-Korteweg, R.C., Ochoa, M., Woudt, P.A., & Andernach, H. 2005a, in “Nearby Large-Scale Structures and the Zone of Avoidance”, ASP Conf. Ser. 329, eds. A.P. Fairall & P.A. Woudt, (San Francisco: ASP), 159 (astro-ph/0406044)
- Kraan-Korteweg, R.C., Staveley-Smith, L., Donley, J., Koribalski, B., & Henning, P.A. 2005b, in “Maps of the Cosmos”, IAU Symp. 216, eds. M. Colless & L. Staveley-Smith, (San Francisco: ASP), in press (astro-ph/0311129)
- Lauberts, A. 1982, The ESO/Uppsala Survey of the ESO (B), (Atlas: ESO, Garching)
- Lucey, J.R., Radburn-Smith, D.J., & Hudson, M.J. 2005, in “Nearby Large-Scale Structures and the Zone of Avoidance”, ASP Conf. Ser. 329, eds. A.P. Fairall & P.A. Woudt, (San Francisco: ASP), 21 (astro-ph/0412329)
- Lundmark, K. 1940, Lundmark Observatory
- Lynden-Bell, D., & Lahav, O. 1988, in “Large-scale motions in the universe”, eds. V.C. Rubin & G.V. Coyne (Princeton, NJ: Princeton University Press), 199
- McHardy, I.M., Lawrence, A., Pye, J.P., et al. 1981, MNRAS 197, 893
- Mamon, G.A. 1998, in “Wide Field Surveys in Cosmology”, eds. Y. Mellier & S. Colombi, (Gif-sur-Yvette: Editions Frontières), 323
- Meyer, M.J., Zwaan, M.A., Webster, R.L., et al. 2004, MNRAS 350, 1195
- Mullis, C.R., Ebeling, H., Kocevski, D.D., & Tully, R.B. 2005, in “Nearby Large-Scale Structures and the Zone of Avoidance”, ASP Conf. Ser. 329, eds. A.P. Fairall & P.A. Woudt (San Francisco: ASP), 183
- Nagayama, T., Ph.D. thesis, Nagoya University, 2004
- Nagayama, T., Woudt, P.A., Nagashima, C., et al. 2004, MNRAS 354, 980

- Nagayama, T., Nagata, T., Sato, S., Woudt, P.A., & IRSF/SIRIUS team 2005, in “Nearby Large-Scale Structures and the Zone of Avoidance”, ASP Conf. Ser. 329, eds. A.P. Fairall & P.A. Woudt (San Francisco: ASP), 177
- Nilson, P. 1973, Uppsala General Catalog of Galaxies, (Uppsala: University of Uppsala)
- Paturel, G., Petit, C., Rousseau, J., & Vauglin, I. 2003, A&A 405, 1
- Peebles, P.J.E. 1994, ApJ 429, 43
- Rousseau, J., Paturel, G., Vauglin, I., Schröder, A., et al. 2000, A&A 363, 62
- Salem, C., & Kraan-Korteweg, R.C., in prep.
- Saunders, W., D’Mellow, K.J., Valentine H., et al. 2000, in “Mapping the Hidden Universe: The Universe behind the Milky Way - The Universe in HI”, ASP Conf. Ser. 218, eds. R.C. Kraan-Korteweg, P.A. Henning & H. Andernach, (San Francisco: ASP), 141
- Schlegel, D.J., Finkbeiner, D.P., & Davis M. 1998, ApJ 500, 525
- Schröder, A., Kraan-Korteweg, R.C., Mamon, G.A., & Ruphy S. 1997, in “Extragalactic Astronomy in the Infrared”, eds. G.A. Mamon, T.X. Thuan & J. Tran Thanh Van (Editions Frontières: Gif-sur-Yvette), 381
- Schröder, A., Kraan-Korteweg, R.C., & Mamon G.A. 1999, PASA 16, 42
- Schröder, A., Kraan-Korteweg, R.C., & Mamon, G.A. 2000, in “Mapping the Hidden Universe: The Universe behind the Milky Way - The Universe in HI”, ASP Conf. Ser. 218, eds. R.C. Kraan-Korteweg, P.A. Henning & H. Andernach, (San Francisco: ASP), 119
- Schröder, A., Kraan-Korteweg, R.C., Mamon, G.A., & Woudt, P.A. 2005, in “Nearby Large-Scale Structures and the Zone of Avoidance”, ASP Conf. Ser. 329, eds. A.P. Fairall & P.A. Woudt (San Francisco: ASP), 167 (astro-ph/0407019)
- Schröder, A.C., Kraan-Korteweg, R.C., & Henning, P.A., in prep.
- Staveley-Smith, L., Wilson, W.E., Bird, T.S., et al. 1996, PASA 13, 243
- Tonry, J.L., & Davis, M. 1981, ApJ 246, 680
- Vauglin, I., Rousseau, J., Paturel, G., et al. 2002, A&A 387, 1
- Vorontsov-Velyaminov, B., Archipova, V.P., & Krasnogorskaja, A. 1962-1974, Morphological Catalogue of Galaxies, Vol. I-V (Moscow: Moscow State University)
- Wakamatsu K., Parker Q.E., Malkan M., & Karoji H. 2000, in “Mapping the Hidden Universe: The Universe behind the Milky Way - The Universe in HI”, ASP Conf. Ser. 218, eds. R.C. Kraan-Korteweg, P.A. Henning & H. Andernach, (San Francisco: ASP), 187
- Wakamatsu, K., Malkan, M.A., Nishida, M.T., Parker, Q.A., Saunders, W., & Watson, F.G. 2005, in “Nearby Large-Scale Structures and the Zone of Avoidance”, ASP Conf. Ser. 329, eds. A.P. Fairall & P.A. Woudt, (San Francisco: ASP), 149
- Woudt, P.A. 1998, Ph.D. thesis, Univ. of Cape Town
- Woudt, P.A., & Kraan-Korteweg, R.C. 2001, A&A 380, 441

- Woudt P.A., Kraan-Korteweg, R.C., & Fairall, A.P. 1999, A&A 352, 39
- Woudt, P.A., Kraan-Korteweg, R.C., & Fairall, A.P. 2000, in “Mapping the Hidden Universe: The Universe behind the Milky Way - The Universe in HI”, ASP Conf. Ser. 218, eds. R.C. Kraan-Korteweg, P.A. Henning & H. Andernach, 203
- Woudt, P.A., Kraan-Korteweg, R.C., Cayatte, V., Balkowski, C., & Felenbok, P. 2004, A&A 415, 9